OPEN ACCESS
Engineering Science & Technology Journal
P-ISSN: 2708-8944, E-ISSN: 2708-8952
Volume 4, Issue 1, P.No. 1-17, March 2023
DOI: 10.51594/estj.v4i1.451
Fair East Publishers
Journal Homepage: www.fepbl.com/index.php/estj

EFFECT OF THE NUMBER OF THE PASSES ON THE MECHANICAL BEHAVIOUR OF ALUMINUM ALLOY PROCESSED USING EQUAL CHANNEL ANGULAR PRESSING (ECAP)

Ahmed.S.M.Agena[1]

University of Zawia-Information Technology Faculty, Libya

*Corresponding Author: Ahmed.S.M.Agena
Corresponding Author Email: ah.agena@zu.edu.ly

Article Received: 01-02-23 **Accepted:** 27-02-22 **Published:** 06-03-23

ABSTRACT

One of the most important industrial processes used in the production of nanomaterials is the ECAP process. Whereby, nanomaterials are produced in relatively large sizes. In this research, the effect of the number of passes on the mechanical behavior of the engineering material was studied. Where the upsetting test was carried out on samples taken from a metal produced by the ECAP process, then the yield stress, maximum stress, and strain values were determined, as well as the Tresca energy fracture criterion was used, and the results were analyzed and converted into graphic relations. From the results, it was found that these values are highly dependent on the number and type of passes.
Keywords: ECAP, Aluminum Alloy, Upsetting Test, Mechanical Properties, Anisotropic.

INTRODUCTION

Equal Channel Angular Pressing (ECAP) process is one of the processes used to produce engineering materials with a nanocrystalline structure. In this process, where the metal is forced to pass through a die containing two channels of equal diameter and intersecting at a specific angle (Baysal, Koçar, Kocaman, & Köklü, 2022). See figure (1).

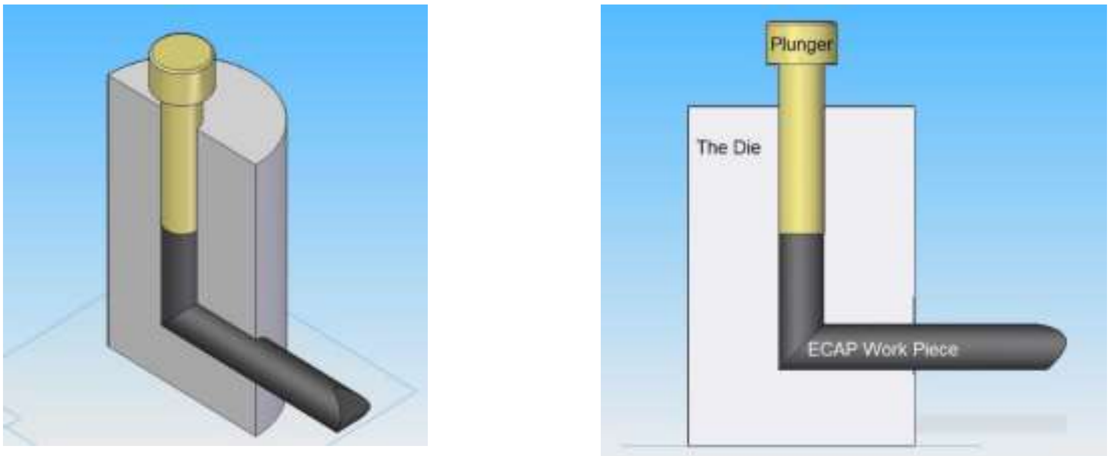

Figure1: The Normal ECAP Process

ECAP is used to cause severe plastic deformation on the bulk material by pure shearing. The basic theory in this process is to apply extreme plastic stress to the material by extruding it inside the channels. The deformation process can be repeated in this process by repeating the extrusion process for the same sample inside the two channels (Valiev, Islamgaliev, & Alexandrov, 2000). The process of re-extrusion of the same sample through the two channels is called passing and is numbered according to the number of passing times. It has three types of routes.

- Route A if the sample is placed in the vertical channel without rotating around its longitudinal axis.
- Routes B and C if the sample rotated around its longitudinal axis by angles of 90º and 180º. Respectively. As shown in Figure (2) (Verlinden, 2005).

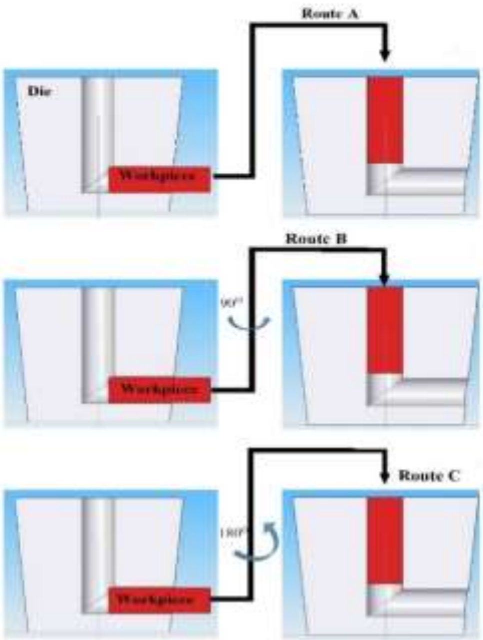

Figure 2: Types of ECAP Routes

This process was developed for producing specific parts suitable for various engineering industries, such as medical industries (vital orthotics) and some components of aircraft and automobile structures. Several types of this process differ in the way they work, but they have the same theory as shown in Figure 3 (L Li and J Virta, 2011).

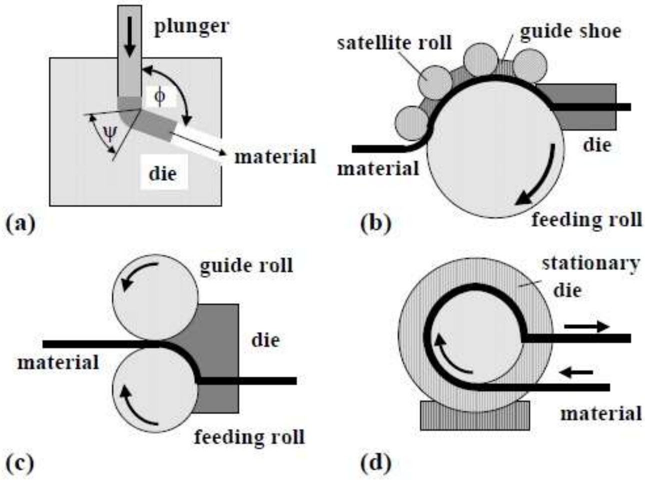

Figure 3: Schematic of: (a)-Equal Channel Angular Pressing (ECAP) Setup, (b)- Conshearing Process, (c), Continuous Confined Strip Shearing, (d)- ECAE-Conform Setup.

Several researchers have studied the effect of the shape and size of the extrusion channels on the mechanical properties of the processed metal (R. Reda, 2019) they dealt with the effect of the intersecting angle between the two channels on the properties of the produced metal.

Researchers have developed a theoretical formula for the amount of deformation (ε) that occurs to the metal after performing the ECAP operation, and it has been found that the amount of this deformation depends on several factors, including the number of times the ECAP operation is performed on the metal (Passes number) and the intersecting angles between the two channels, as shown in Equation (1) (Iwahashi, Wang, Horita, Nemoto, & Langdon, 1969), (Anibal, Prados, Valio, Rubert, Sordi, & Ferrante, 2011), (Vedani, Bassani, Tuissi, & Angella, 2004).

$$\varepsilon_n = N\left[\frac{2\cot\left(\frac{\phi}{2}+\frac{\psi}{2}\right)+\psi\,\mathrm{cosec}\left(\frac{\phi}{2}+\frac{\psi}{2}\right)}{\sqrt{3}}\right] \tag{1}$$

Where

N is the number of passes.

$\emptyset$ and ψ are the inner and outer intersecting angles between the two channels, as shown in Figure (4)(Mohan, Tyagi, and Dixit, 2020).

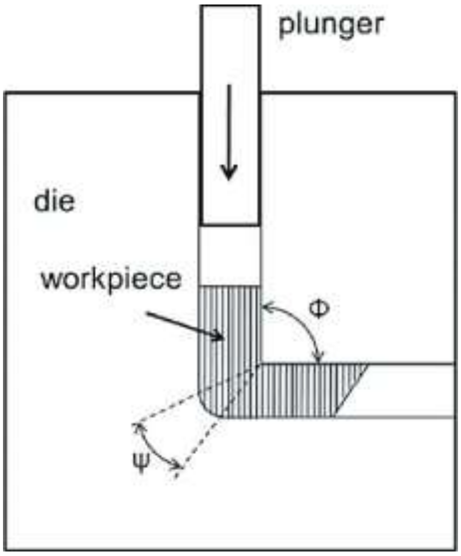

Figure 4: Principle of ECAP Showing Channel Angle $\emptyset$ = 90º and Curve Angle ψ

Another study investigated the effect of the inner intersecting angle ($\emptyset$) value between the two channels, where they used dies with channels intersecting at different angles ranging from 90º to 135º , (see figure 5)(Agarwal, & Tyagi, 2017), (Fadhil, Alkhfaji, & Ismael, 2021).
ECAP process was carried out on different types of metals such as aluminum alloys (Agena, 2009), copper (Vijayashakthivel, Dath., & Krishnamurthy, 2014), titanium (Agarwal, Tyagi, Singhal, & Bhatia, 2020), steel (Irfan, & Omar, 2019), etc., at temperatures lower than the recrystallization point.
In this work, the heterogeneous and anisotropic properties of aluminum alloy processed by the ECAP were studied. Where the intersecting angle between the two channels was equal to 90^{O}, the ECAP process was carried out at room temperature.

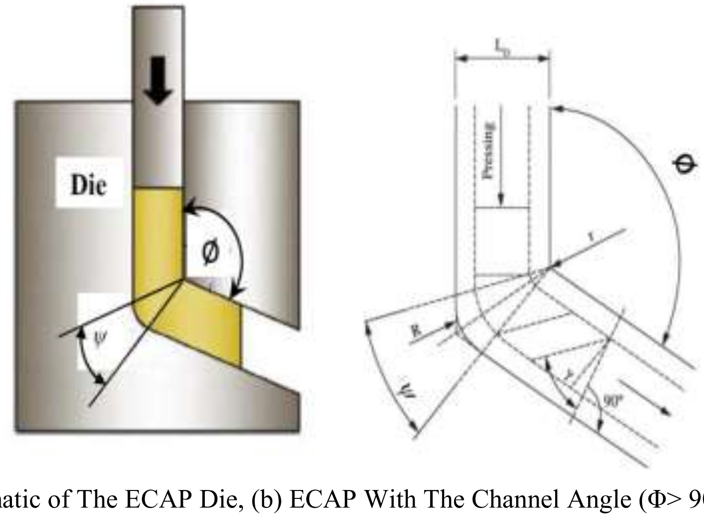

Figure 5: (a) Schematic of The ECAP Die, (b) ECAP With The Channel Angle (Φ> 90º) and Outer Arc Angle (Ψ)

The aim of this study is to find out the relationship between the number of passes and the change in the mechanical properties of aluminum alloy 6082.

EXPERIMENTAL METHOD

Materials Preparation

Al - 6082 alloy material was processed by equal channel angular pressing (ECAP), the chemical composition of this alloy is given in table (1).

Table1: Chemical Composition of Al-6082 Alloy (wt %)

Al	Cr	Cu	Fe	Mg	Mn	Si	Ti	Zn
95.2	0.25	0.1	0.5	0.6	0.4	0.7	0.1	0.2

Workpieces were subjected to one, four, and eight ECAP passes using route **C** at room temperature. Attaching a Cartesian coordinate system to the workpiece, three cylindrical and flanged samples (see figure 6) were extracted from the ECAP piece in the direction of the three Cartesian axes.

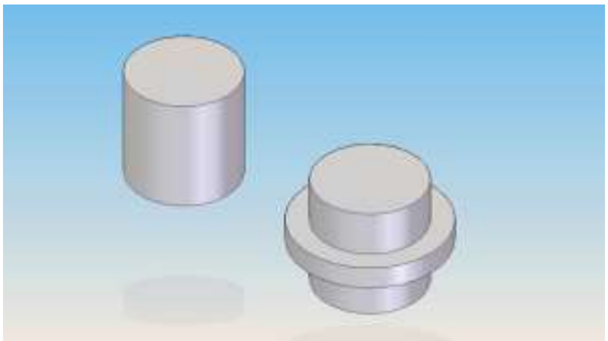

Figure 6: Cylindrical and Flanged Specimens

Each sample was taken from the direction of a specific axis, in order to conduct mechanical tests on it. These samples were taken from all types of specimens produced by the ECAP process. These directions were:

The 'longitudinal' direction was equal to the longitudinal axis of the workpiece.

The '0°' direction was equal to the vertical direction of the punch movement during formation.

And the '90°' direction was perpendicular to the previous and the longitudinal directions, as shown in figure (7). The dimensions of the samples on which the upsetting test was carried out in this research are shown in Figure (8).

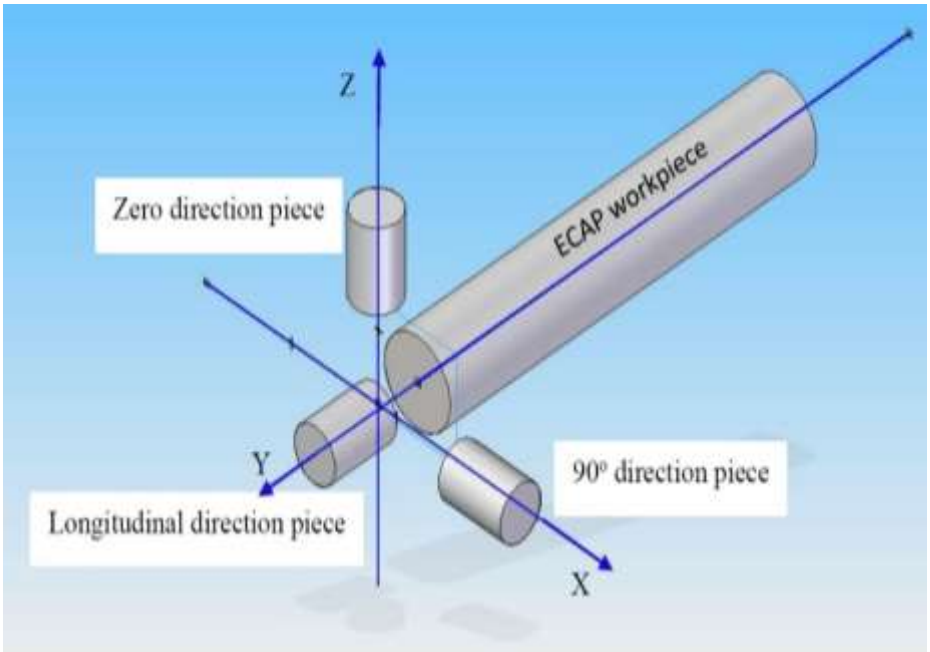

Figure 7: ECAP Workpiece and the Direction of Specimen Axes for Upsetting Test

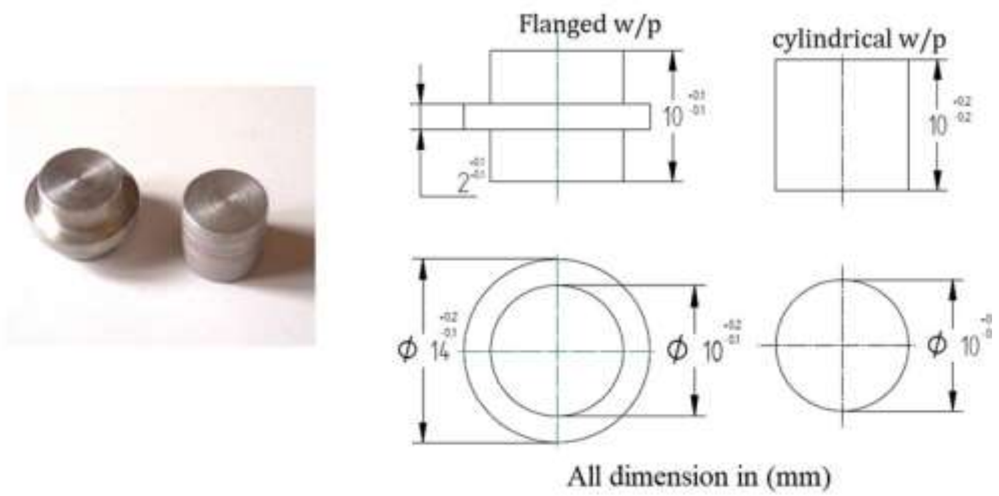

Figure.8. Dimensions of Cylindrical and Flanged Specimens

Cold Upseting Test

Most metalworking processes involve compressive deformation, and so the uniaxial compression test has been widely used for studying deformation behavior.

During compression in the upsetting test, the cylindrical sample turns into a bulging barrel shape due to the friction between the upper and lower sample surfaces and the die surface. This results in an increase in deformation and true of the metal in the mid-height region of the sample more than the area in contact with the two surfaces of the die.

Collectively, the cylindrical and flanged compression–test specimens provide a wide range of circumferential tension/axial compression strain states.

During the upsetting test, cylindrical and coller (flanged) specimens were deformed in several steps until cracks appeared. It was observed that the initial circular cross-section of the specimens became elliptical during upsetting (Figure 9), this means that unequal and inhomogeneous deformation occurs in different directions of the sample, which is known as anisotropic deformation.

(a) **(b)**

Figure 9: The Specimens After the Upsetting Test: (a) Cylindrical Pieces, (b) Flanged Pieces

Determination of True Curves

During performing the upsetting process, the force applied to the cylindrical sample was recorded and the amount of decrease in the height of the sample was measured at each stage.

Then the true stress and true strain were calculated, For all samples taken from the ECAP piece and in all directions (Ahmed S.M. Agena, 2009). The following equations were used in the calculation:

The true stress σ_i and the true strain ε_i are:

$$\sigma_i = \frac{P_i}{A_i} \tag{2}$$

$$\varepsilon_i = \ln \frac{h_0}{h_i} \tag{3}$$

where P_i is the instantaneous force and A_i is the instantaneous area, which can be calculated from volume constancy as

$$A_i = \frac{A_0}{h_i} h_0 \tag{4}$$

where A_0 is the initial area of the specimen, h_i is the initial high of the specimen, and h_i is the instantaneous high of the specimen.

From the calculation, the true stress-true strain curves of all specimens were plotted as shown in Figure (10) (Ahmed S.M. Agena, 2009).

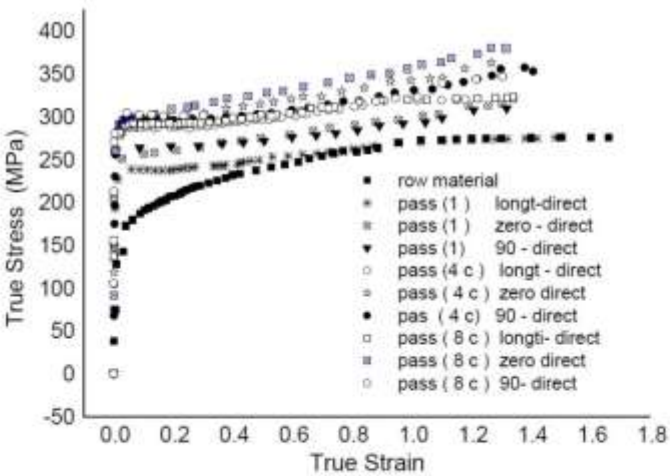

Figure10: True Stress-True Strain Curves for All Types of Specimens

These results have been published in our previous research. However, in this work, we will reinvestigate these results and analyze them to find the relationship between the different types of passes of the ECAP piece and the change in the mechanical properties of the resulting metal, and try to understand what happens in the metal.

Usually, the (ECAP) process produces bulks of nanostructured materials, where the mechanical properties and workability of the materials produced by this process depend on the number of passes, the type of route, and the direction of the sample axis.

Ductile Fracture Criteria

The workability characteristic of these materials refers to the relative ease with which the material can be formed and the extent of its plastic deformation. It is a function of material and process. Greater workability of the material allows greater deformation.

There are several tests that can be performed currently to evaluate the ductility of nanostructured materials such as tension, torsion, and compression tests. The initiation of ductile fracture is a major factor affecting the deformation limit in many metalworking processes.

In this work, several upsetting tests were carried out to evaluate the formability of nanostructured Al -6082 alloy by using flanged specimens (Figure 8). Tresca Energy criterion was chosen to determine the limit of the bulk deformation. The empirical formula of this criterion is described below:

Tresca Energy Fracture Criterion

This is a simple criterion. Considering the difference between tensile and compression stresses, and is as follows:

$$\frac{1}{\sigma_y}\int_0^{\overline{\varepsilon_f}}\left(\frac{\sigma_1-\sigma_2}{2}\right)d\bar{\varepsilon}=C1 \qquad (5)$$

Where σ_1 is the maximum tensile stress, σ_2 is the maximum compression stress and σ_y is the yield stress.

C_1 is a constant.

This ductile fracture criterion needs to calculate the stress state and effective strain.

RESULT AND DISSCTION

Using the Origin program, the true stress and strain curves were analyzed for all samples to find the best mathematical formula that matches and fits these curves as shown in Figure (11).

It was found that the best mathematical formula that represents and applies to these curves is similar to the ***Holloman*** power law equation, which is expressed in the following formula:

$$\sigma = K\varepsilon^n \qquad (6)$$

Where σ is the true stress, K is the strength coefficient, n is the strain hardening coefficient and ε is the true strain.

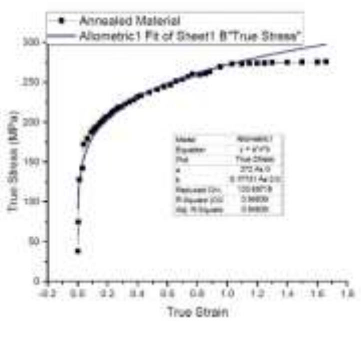

Figure 11-a: The Fit Curve for Annealed Material

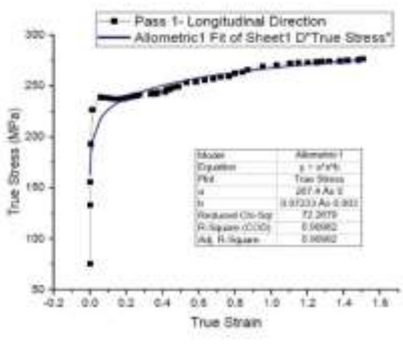

Figure 11-b: The Fit Curve for Pass 1-Longitudinal Direction

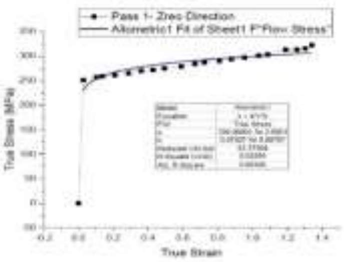

Figure 11-c: The Fit Curve for Pass 1-Zero Direction

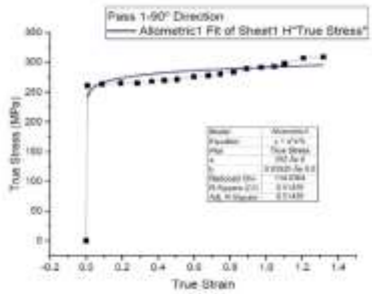

Figure 11-d: The Fit Curve for Pass 1-90° Direction

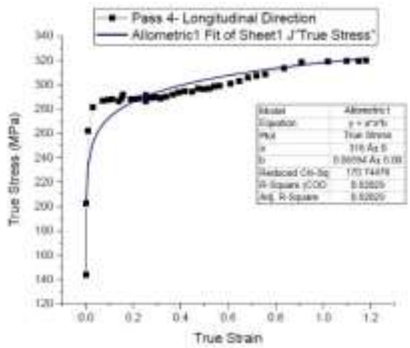

Figure 11-e: The Fit Curve for Pass 4-Longitudinal Direction

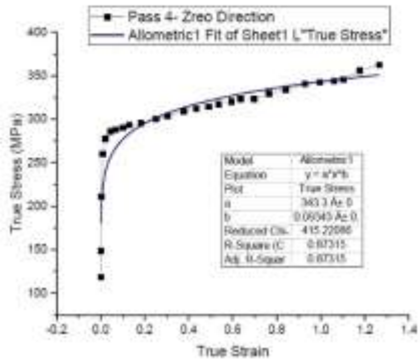

Figure 11-f: The Fit Curve for Pass 4-Zero Direction

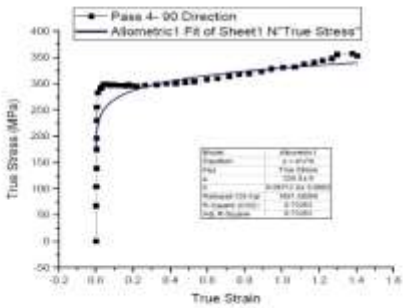

Figure 11-g: The Fit Curve for Pass 4-90° Direction

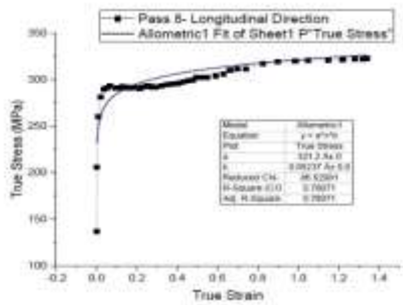

Figure 11-h: The Fit Curve for Pass 8-Longitudinal Direction

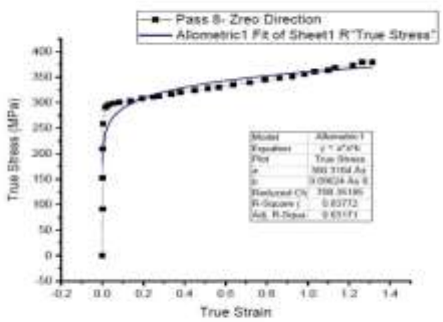

Figure 11-i: The Fit Curve for Pass 8-Zero Direction

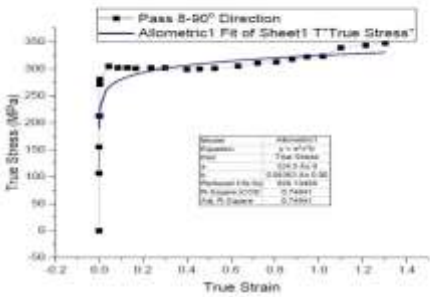

Figure 11-j: The Fit Curve for Pass 8-90° Direction

From the analysis process, the Holloman power law equation constants values were determined for all types of samples. The results are shown in Table (2):

Table 2 : The Value of Constants of Holloman Power Law Equation for All Types of Samples

No of pass	σ_y (MPa)	K (MPa)	n
Annealed material	172	272.307	0.1777
1 -longitudinal	240	267.4	0.07233
1-zero direction	250	298.3	0.07307
1-90° direction	260	292	0.039
4c- longitudinal	285	318	0.065
4c-zero direction	288	343.4	0.09343
4c-90° direction	300	330	0.087
8c- longitudinal	290	321.2	0.0523.
8c-zero direction	300	358.4	0.0962
8c-90° direction	305	324.5	0.06363

From the above table, it is possible to find and draw the relationship between the pass number (sample type) and the value of the different constants of the Holloman power law equation, as shown in the following curves.

The Yield Stress

From the obtained results, the relationship between the pass number and the yield stress for all directions can be drawn as shown in the figures. (12).

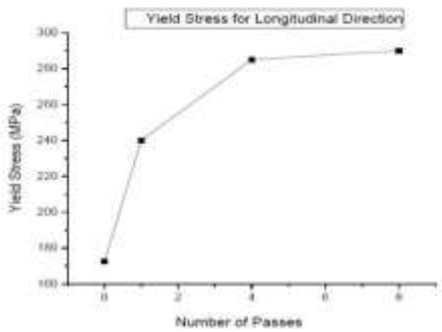

Figure 12-a: The Relationship Between Passes Number and Yield Stress for The Longitudinal Direction

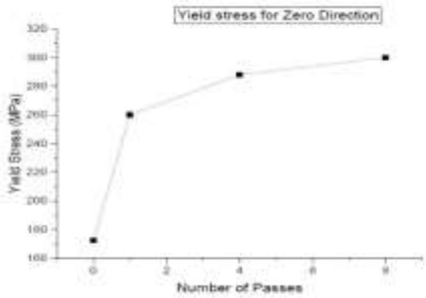

Figure 12-b: The Relationship Between Passes Number and Yield Stress for The Zero Direction

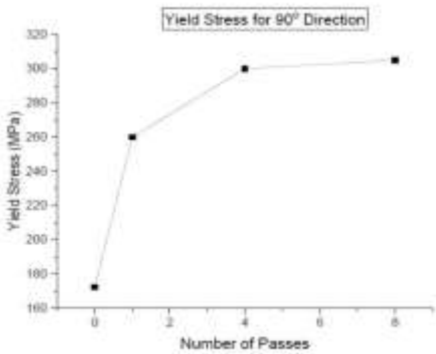

Figure 12-b: The Relationship Between Passes Number and Yield Stress for The 90° Direction

From the curve, we notice that when the pass number increased, the amount of yield stress increased too, and we notice that the curves take the form of an exponential curve, which prompted us to find the type of exponential curve that applies to each case.
By using the Origin program, the fitting curve (red lines) was found for each of the previous cases of relationships, so that this curve touches most of the points, the following empirical exponential equation was used to draw the fitting curves as shown in the figure (13).

$$y = y_0 + A \times e^{\frac{-x}{b}} \tag{7}$$

Where:
y = the yield stress of certain pass number, y_0 = the yield stress of row material, x = number of passes, and A, b = constants.

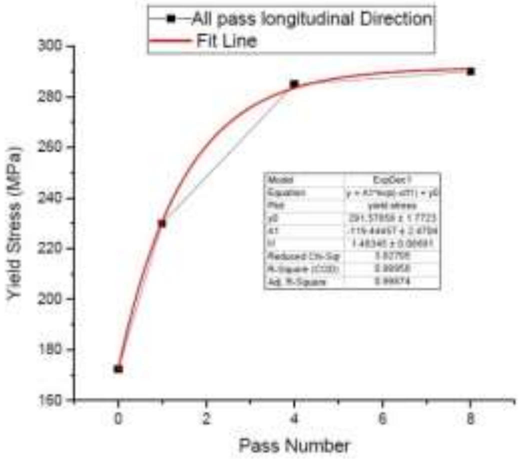

Figure 13-a: The Yield Fitting Curve for The Longitudinal Direction

Figure 13-b: The Yield Fitting Curve for The Zero Direction

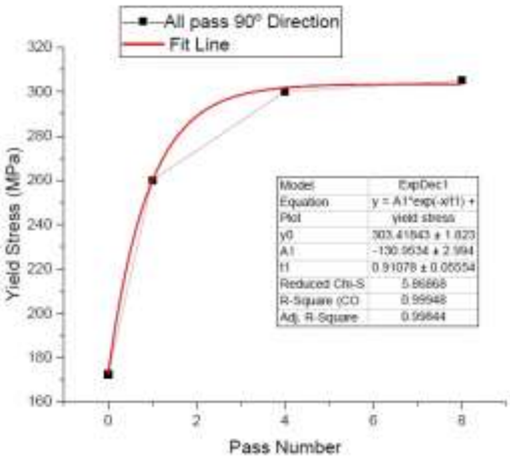

Figure 13-c: The Yield Fitting Curve for The 90° Direction

From the analysis of the data of the fitting curves, the values of the variables were found for each case. As shown in table (3).

Table 3: Variables of Yield Fitting Curve Values

Direction type	y_0	A	b
Longitudinal Direction	291.6	-119.44	1.48
Zero Direction	294.63844	-123.0	1. 0348
90º Direction	303.41843	-130.9534	0.91078

From fitting curves extracted from the data analysis process, it is possible to predict the estimated yield stress values for the new cases of other passes such as the yield stress of pass number two, three, five, six, and seven.

The Strength Coefficient (K- Coefficient)

K is a constant known as the Strength Coefficient, defined as the true strength at a true strain of 1.

From table1, the relationship between the pass number and the K- coefficient (Strength Coefficient) for all directions can be drawn as shown in the figures (14).

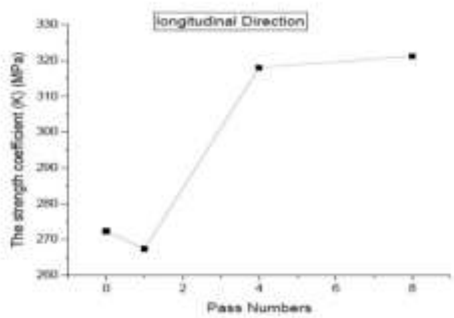

Figure14-a: The *K*- Coefficient for The Longitudinal Direction

Figure14-a:. The K- Coefficient for The Zero Direction

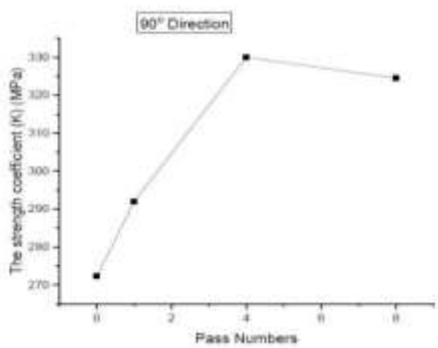

Figure14-a: The K- Coefficient for The 90º Direction

It is quite noticeable that the K- Coefficient values are fluctuating. For the samples taken from the longitudinal direction, the value of the *K*- Coefficient of annealed material is greater than that in pass l and keeps rising. In the case of the samples taken from zero direction, the K- Coefficient starts to rise to reach its highest value in pass 8, whereas, for samples taken from the direction of 90°, the value starts to rise, to reach its highest value in pass 4 before they start to descend in pass 8.

The Strain-Hardening Coefficient (*n*- coefficient)

From table 1, the relationship between the pass number and the strain-hardening coefficient (*n*-coefficient) for all directions can be drawn as shown in the figures (15).

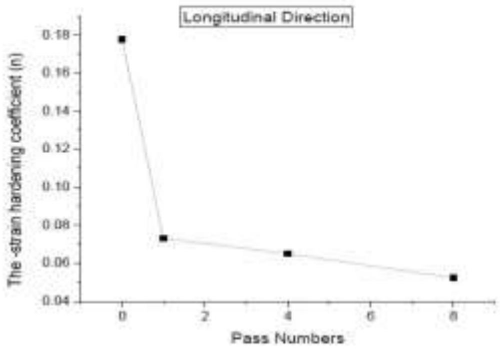

Figure15-a: The n - Coefficient for The Longitudinal Direction

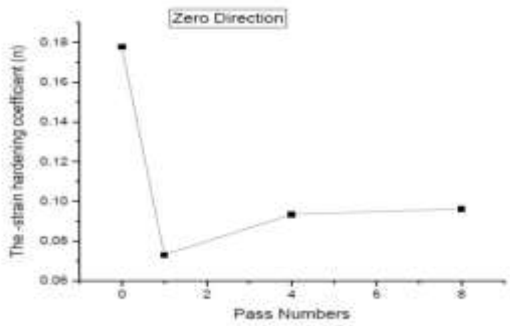

Figure15-b: The n - Coefficient for The Zero Direction

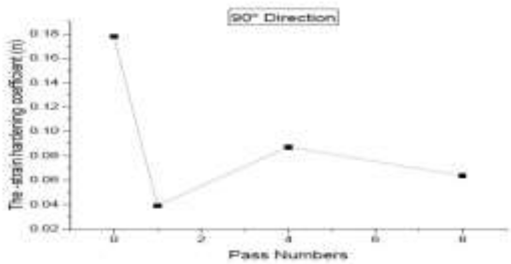

Figure15-c: The n - Coefficient for The 90° Direction

It can be noted that the strain-hardening coefficient (*n*- coefficient) values also fluctuate. Whereas, in the case of samples taken from the longitudinal direction, the value of the *n*-coefficient is decreasing. While in the case of the samples taken from the zero and the 90° directions, it was noted that the values of the *n*- coefficient start to decrease up to pass 1 then rise again at pass 4 and decrease at pass 8.

Maximum True Stress

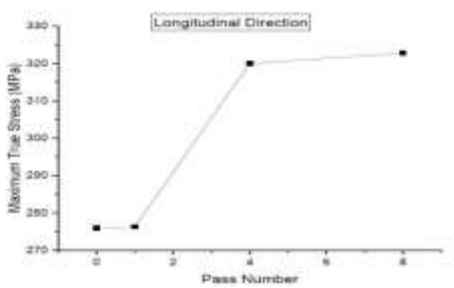

Figure16-a: Maximum True Stress for The Longitudinal Direction

Figure16-a: Maximum True Stress for The Zero Direction

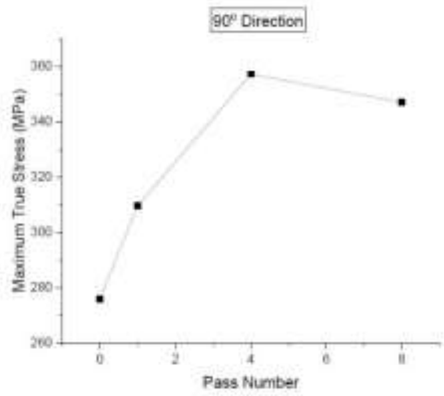

Figure16-a: Maximum True Stress for The 90° Direction

The maximum true stress curves show that the maximum true stress values are equal in annealed material (represented by number 0, in the horizontal axis) and pass 1, and then keeps rising in the case of samples taken from the longitudinal direction.

While in the case of the samples taken from the zero direction, we notice that the value of the maximum true stress keeps rising, reaching the highest value at pass 8.

In the case of samples taken from direction 90°, we notice that the value of the maximum true stress starts to rise, reaching the highest value in the case of pass 4, and then descends in pass 8. However, the value of the maximum stress in the case of pass 8 remains greater than the value in the case of pass 1 and the row material.

Maximum True Strain

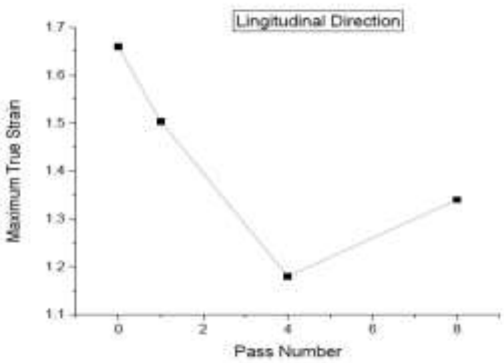

Figure17-a: Maximum True Strain for The Longitudinal Direction

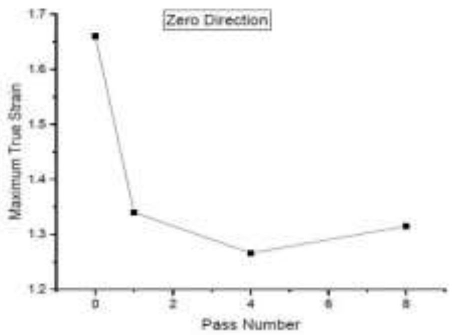

Figure17-b Maximum True Strain for The Zero Direction

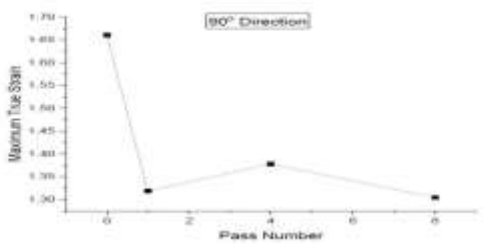

Figure17-c: Maximum True Strain for The 90° Direction

The curves of the maximum strain show that the largest value of the maximum strain is in the case of the annealed metal (represented by 0 number on horizontal axis).

In the case of samples taken from the longitudinal and zero directions, the values of the maximum strain start decreasing until it reaches pass 4 metal, then it goes up a bit in the case of pass 8 metal.
While in the case of the samples taken from the 90° direction, we notice that the values of the maximum true strain start to rise a bit in the case of pass 4 metal, and then it goes down at pass 8.

Tresca fracture constant

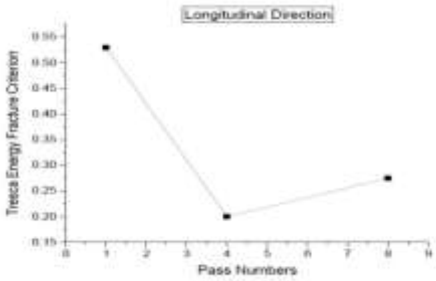

Figure18-a: Tresca Fracture Constant for The Longitudinal Direction

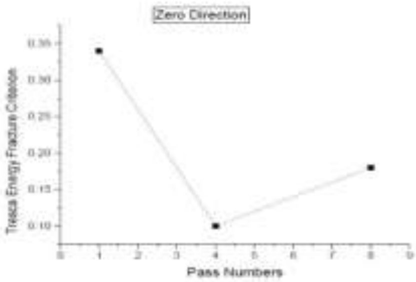

Figure18-b: Tresca Fracture Constant for The Zero Direction

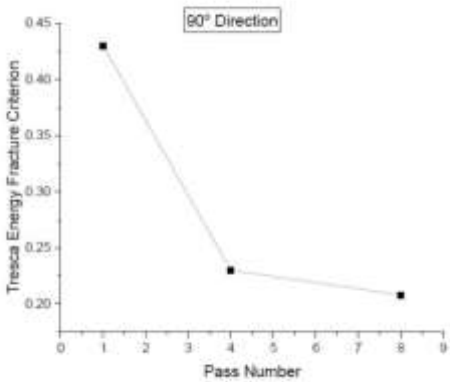

Figure18-c: Tresca Fracture Constant for 90° Direction

We can see that the Tresca fracture constant values are fluctuating too. Whereas, in the case of samples taken from the longitudinal and the zero directions the value of the Tresca fracture constant decreases until it reaches pass 4 and then begins to rise again at pass 8.
While in the case of the samples taken from the 90° direction, we notice that the values of the Tresca fracture constant decrease until it reaches pass 8.

CONCLUSION

1. In this work, the effect of the number of passes on the mechanical properties of an aluminum Al-6082 Alloy worked by ECAP was studied. From the results, the following are the conclusions:
2. Using the Origin program, the true stress curves were analyzed for all samples to find the best mathematical formula that matches and fits these curves.
3. It was found that the best mathematical formula that represents and applies to these curves is similar to the Holloman power law equation, the Holloman power law equation constants values were determined for all types of samples.

4. It observed that, when the pass number increase, the amount of yield stress increase too, and It was noted that the curves take the form of an exponential curve, which prompted us to find the type of exponential curve that applies to each case.
5. It is quite noticeable that the K- Coefficient values are fluctuating, on the longitudinal and the zero directions, the K- Coefficient starts to rise to reach its highest value in pass 8, whereas, for samples taken from the direction of 90o, the value starts to rise, reaching its highest value in pass 4.
6. It can be noted that the strain-hardening coefficient (n- coefficient) values also fluctuate. In the longitudinal direction, the value of the n- coefficient is decreasing. While in the case of the samples taken from the zero and the 90o directions, it was noted that the values of the n-coefficient start to decrease up to pass 1 then rise again at pass 4 and decreases at pass 8.
7. In longitudinal and zero directions, we notice that the values of the maximum true stress keep rising, reaching the highest value at pass 8. However, in the case of samples taken from direction 90o, the values of the maximum true stress start to rise, reaching the highest value in the case of pass 4 and then descending in pass 8.
8. The curves of the maximum strain show that the largest value of the maximum strain is in the case of the annealed metal (represented by 0 number in the horizontal axis).
9. It is quite noticeable that the Tresca fracture constant values fluctuate too.
10. All previous results indicate that the aluminum alloy has acquired inhomogeneous properties, which is known as anisotropic behavior.

References

Agarwal, K.M., & Tyagi, R.K. (2017). Investigation of mechanical properties of metals and alloys processed after equal channel angular pressing. *AGU International Journal of Engineering Technolology, 5,* 53–65.

Agarwal, K.M., Tyagi, R.K., Singhal, A., & Bhatia, D. (2020). Effect of ECAP on the mechanical properties of titanium and its alloys for biomedical applications. *Materials Science for Energy Technologies, 3,* 921-927. https://doi.org/10.1016/j.mset.2020.11.002

Agarwal, M.K., Yyagi, R.K., & Dixit, A. (2020). Theoretical analysis of equal channel angular pressing method for grain refinement of metals and alloys. *Materials Today Proceedings, 25*(4), 668-673. https://doi.org/10.1016/j.matpr.2019.08.026

Ahmed S.M., & Agena.(2009). A study of flow characteristics of nanostructured Al-6082 alloy produced by ECAP under upsetting test. *Journal of Materials Processing Technology, 209*(2 856-863. https://doi.org/10.1016/j.jmatprotec.2008.02.081

Baysal, E., Koçar, O., Kocaman, E., & Köklü, U.(2022). An overview of deformation path shapes on equal channel angular pressing. *Metal, 12,* 1800. https://doi.org/10.3390/met12111800

Fadhil, A., AlKhfaji, S.S., & Ismael, M.K. (2021). Design parameters for equal-channel angular pressing (ecap) via numerical approach. *Journal of Physics: Conference Series 1973, 012103,* https://doi:10.1088/1742-6596/1973/1/012103

Filho, A.D.A.M., Prados, E.F., Valio, G.T., Rubert, J.B., Sordi, V.L., & Ferrante, M. (2011). Severe plastic deformation by equal channel angular pressing: product quality and operational details. *Material Research*, *14*(3), 335–339. https://doi:10.1590/S1516-14392011005000045

Irfan, O.M., & Omar, H.M.(2019). Influence of grain refinement by ecap on mechanical and erosion corrosion properties of AISI 4130 Steel: Experimental and Prediction Approach. *Metallurgical and Materials Transaction*, *50*, 4232–4244. https://doi.org/10.1007/s11661-019-05339-1

Iwahashi, Y., Wang, J., Horita, M., Nemoto, M., & Langdon, T.G. (1996). Principle of equal-channel angular pressing for the processing of ultra-fine grained materials. *Scripta Mater*, *35*(2), 143-146.

Leijun, L.I., & Virta, J. (2011). Ultra-high strength steel wires processed by severe plastic deformation for ultrafine grained microstructure. *Materials Science and Technology*, *27*(5), 845-862, DOI:10.1179/026708310X12677993662087

Reda, R. (2019). Equal Channel Angular Pressing (ECAP): die design, processing handicaps and mechanical characterization. *Evolution of Mechanical Engineering*, 2(5), 1-7. Retrieved from https://crimsonpublishers.com/eme/fulltext/EME.000547.php

Valiev, R.Z., Islamgaliev, R.K., & Alexandrov, I.V. (2000). Bulk nanostructured materials from severe plastic deformation. *Progress in Material Science, 45*, 103-189.

Vedani, M., Bassani, P., Tuissi, A., Angella, G. (2004). Ultrafine grained alloys produced by severe plastic deformation: issues on microstructural control and mechanical behavior. Presented at the “2nd International Conference & Exhibition in Metallurgical Process Technology”, Riva del Garda 19-21 Sett.

Verlinden, B. (2005). Severe plastic deformation of metals. *Metalurgija – Journal of Metallurgy, 11*(3), 165-182.]

Vijayashakthivel., A. T., Srikantha Dath., A. T., & Krishnamurthy. R. (2014). Response of copper to Equal Channel Angular Pressing with different processing temperature. *Procedia Engineering, 97* , 56-63. https://doi.org/10.1016/j.proeng.2014.12.224